5-15-1989

Stochastic Evolution of Refractory Interstellar Dust During the Chemical Evolution of a Two-Phase Interstellar Medium

Kurt Liffman
Rice University

Donald D. Clayton
Clemson University, claydonald@gmail.com

THE ASTROPHYSICAL JOURNAL, 340:853–868, 1989 May 15

STOCHASTIC EVOLUTION OF REFRACTORY INTERSTELLAR DUST DURING THE CHEMICAL EVOLUTION OF A TWO-PHASE INTERSTELLAR MEDIUM

KURT LIFFMAN[1] AND DONALD D. CLAYTON
Department of Space Physics and Astronomy, Rice University
Received 1988 August 22; accepted 1988 October 27

ABSTRACT

We present a study of the evolution of refractory interstellar dust designed to clarify the possibilities for systemic behavior. The study is embedded in an analytic solution of the bulk chemical evolution of a two-phase interstellar medium in which stars are born in molecular clouds but new nucleosynthesis products and stellar return are entered into a complementary diffuse medium. The well-mixed matter of each interstellar phase is repeatedly cycled stochastically through the complementary phase and back. Refractory dust is created by thermal condensation as stellar matter flows away from the supernova sites of nucleosynthesis (in SUNOCONs) and/or from the matter returned from evolved intermediate stars (in STARDUST). This dust is studied on a particle-by-particle basis as it is sputtered by shock waves in the diffuse medium, accretes an amorphous mantle of gaseous refractory atoms while its local medium joins the molecular cloud medium, and encounters the possibility of astration within molecular clouds. The history of each particle is traced by standard Monte Carlo techniques. We present results relevant to these (and other) issues: the size spectrum of interstellar dust; its spectrum of structural distributions between thermally condensed cores and amorphous accreted mantles; its age spectrum and the distinction among its several lifetimes; depletion factors of refractory atoms in the diffuse gas; and isotopic anomalies.

Subject headings: galaxies: evolution — interstellar: abundances — interstellar: grains — nucleosynthesis — numerical methods

I. INTRODUCTION

We calculate in this work numerical models of the evolution of refractory dust in the interstellar medium. The complications and unknowns in such a problem are daunting. For definiteness we will make many specific assumptions that, taken together, define a tractable model of both dust structure and interstellar matter evolution. By solving this model, we hope to learn how such systems behave and to explicate features of them that remain fuzzy in the absence of quantitative modeling. Such detailed solutions have not, to our knowledge, previously apppeared in the literature. On top of that general objective, we point toward answers to these questions: (1) What particle-size spectrum is generated by cycles of sputtering and reaccretion? (2) What magnitudes of gas depletion and differential depletion of different elements are generated by such models? (3) If thermal condensation of isotopically special condensates occurs within expanding supernova interiors (the SUNOCONs defined by Clayton 1978), what fraction of these persists until the time of formation of the solar system's meteorites in which the isotopic anomalies are found? (4) What distinction should be made between the lifetimes of particles defined as the durations of their existence as entities and their mass-sputtering lifetimes defined as a mean time for removing mass from particles by sputtering? These questions and others motivate this study, which is the second such work in our program addressing this topic. Liffman and Clayton (1988) presented detailed results of a similar investigation, but with a different computational scheme based on Monte Carlo histories for independent single particles. The present work casts the calculation into a time-dependent mass-conserving framework for the chemical evolution of the Galaxy. As such it is a more satisfying astrophysical calculation, but more demanding of the computer.

The simplifications of the astrophysical setting that we make in order to facilitate a calculation are the same as those made by Liffman and Clayton (1988). Because both the interstellar medium and the migration of material among its phases are so complicated and still poorly understood, we approximate them by a two-phase medium in which material changes phase abruptly but randomly. The two phases are herein described as *diffuse clouds* and *molecular clouds.* Because these two real phases do comprise almost all of the interstellar mass in the Galaxy, we regard the other phases as short-lived transitional ones that we neglect for simplicity. The warm intercloud gas in that context is regarded as a short-lived subphase of the diffuse clouds. Our calculation will take all star formation as occurring in the molecular clouds; however, we assume that the star formation occurs in associations that disrupt the molecular cloud at the position of the burst of star formation, so that the material ejected from those stars will be returned to the diffuse clouds (perhaps via a neglected and transitional hot phase). This process randomly selects portions of the molecular cloud medium and places them into the diffuse cloud portion. This mass transfer is opposed by the processes by which the diffuse cloud matter is added to the molecular clouds. Although we imagine this physically happening either by diffuse clouds physically joining a preexisting molecular cloud or by the creation of a new molecular cloud by a cooling phase transition, we describe it in our program simply as a random selection of diffuse material to add to the molecular material. We maintain no other description of these phases at this level of formulation, so that we do not distinguish between a large number of clouds at the one extreme or a single cloud of each medium at the other extreme. Operationally our calculation has only the two media masses and the migration of material

[1] Present address: NASA Ames Research Center.

between them. This migration is controlled by two parameters representing the lifetimes of material in each phase against transferral to the other phase. In the calculation itself we take $\tau = 10^8$ yr for both transferral lifetimes on the grounds that equal masses of each coexist at the solar galactocentric distance. These lifetimes have the usual statistical meaning. Some particles reside longer, some less, than τ before transferral. We think of the particles as mixing randomly in each phase, so that in a time increment dt the probability dP that a given particle resides in one of the mass elements transferring during interval dt is $dP = dt/\tau$. This essentially recovers the single-particle Monte Carlo approach of Liffman and Clayton (1988); but by calculating the mass balance of the gas in a time-dependent way we are able to follow the reaccretion of the gas in a time-dependent way.

Refractory gas exists only in the diffuse medium of our simplified model, for two reasons: (1) sputtering of dust occurs only in the diffuse medium (by assumption); (2) return of gas from stars is assumed to be into the diffuse medium only, even though the stars were born within molecular clouds. This gas is subsequently reaccreted by particles in our calculation when they transfer to molecular clouds. Any accretion during diffuse cloud residence is countermanded by the larger average rate of sputtering there, so that our calculation subsumes such accretion under an adjusted mean sputtering rate. We assume that refractory atoms stick when they hit a grain during the transfer process. A key to our calculation lies in our description of this accretion process. We envision gas and particles to be well mixed in the diffuse phase, but to maintain a uniform dust-to-gas ratio. When a mass element $dM_{\rm DC}$ of the diffuse cloud mass $M_{\rm DC}$ joins the molecular phase, the particles within $dM_{\rm DC}$ accrete by assumption the well-mixed gaseous atoms of refractory elements contained within $dM_{\rm DC}$. Because they do this in proportion to the surface areas of those particles, it follows that each particle accretes the same thickness Δr of new refractory mantle (Clayton 1980). Because we will know in our calculation the mass of refractory condensable gas per particle, we will be able to calculate $\Delta r(t)$ as it evolves. And because we do this within a calculation of the chemical evolution of the Galaxy, we are also able to follow the growth of metal abundances.

We use the adjective *refractory* because we emphasize that portion of dust that may condense thermally during the expansions of supernova interiors (SUNOCONs) or during hot outflows from stars (STARDUST). We calculate no chemistry, however. We envision a suite of common abundant mineral-forming elements (Al, Ca, Ti, Fe, Mg, Si) that are known to be condensed at $T > 1000$ K in thermal equilibrium (Grossman and Larimer 1974), and we specify the fraction of that suite that condenses within SUNOCONs following their initial nucleosynthesis when they are isotopic tracers and the fraction that condenses within STARDUST when material is returned to the interstellar medium (ISM) from evolved stars. In our initial survey of results to be reported here, we will describe three limiting cases for those condensation efficiencies: (1) 100% of these elements condense initially into SUNOCONs but the return from stars is gaseous; (2) 50% of these elements condense in SUNOCONs but the return from stars is gaseous; (3) 100% of these elements condense both in SUNOCONs and in STARDUST from the stellar return. These cases are adequate to establish a sense of the possibilities.

Because the chemical fractionations are of interest even though we do not calculate them here, we represent the refractory sequence as Liffman and Clayton (1988) did by supposing that the thermally condensed SUNOCONs and STARDUST have a superrefractory phase A core (which we think of as Al_2O_3 and its associated minerals) surrounded by a refractory phase B mantle (which we think of as $MgSiO_3$ and other silicates). This refractory sequence has been much discussed in geophysics (Grossman and Larimer 1974) and is accompanied by interesting trace-element patterns. We will arbitrarily take these refractory phases to have relative mass $m_B/m_A = 7$ in each condensate, primarily for the simplicity of the initial ratio of radii $r_B/r_A = 2$ of mantle to core in each particle, but also because that ratio is close to the mass ratio $MgO:Al_2O_3$. The advantage of specifying this structure for the injected thermal condensates is that we will be able to calculate the differential destruction by sputtering of these two phases owing to the shielding of the phase A superrefractory cores by the refractory phase B mantle and by the amorphous second mantle (phase C) produced by the reaccretion of gaseous refractory atoms while the particles' transit cloud leaves the sputtering medium. Our code will inject these particles into the diffuse medium and then follow the random walks of their subsequent histories, keeping track of the core mass m_A, thermally condensed mantle mass m_B, and accreted mantle mass m_C. A schematic sample of such particles is illustrated in Figure 1.

We choose to do all of this within a simple model of the chemical evolution of the ISM. Therefore we first describe how that theory provides a quantitative framework for the dust injection rates before returning to more details relevant to the particles themselves.

II. BULK ABUNDANCE EVOLUTION

It is significant for the refractory particle content that the *concentration* of refractory metals increases in the interstellar content of both phases. To this end we begin with analytic solutions of the chemical evolution of a two-phase ISM. With the assumptions stated above, the total masses of the diffuse and molecular phases satisfy

$$\frac{dM_{\rm MC}}{dt} = -\psi(t) + \frac{M_{\rm DC}}{\tau_{\rm DC}} - \frac{M_{\rm MC}}{\tau_{\rm MC}} \tag{1}$$

and

$$\frac{dM_{\rm DC}}{dt} = E(t) + \frac{M_{\rm MC}}{\tau_{\rm MC}} - \frac{M_{\rm DC}}{\tau_{\rm DC}} + f(t)\,, \tag{2}$$

where we will as simplifications employ $\tau_{\rm DC} = \tau_{\rm MC} = 10^8$ yr for the interphase transfer rate, will take the total ejecta from stars to be given by the instantaneous recycling approximation $E(t) = R\psi(t)$, where R is the return fraction and $\psi(t)$ the star formation rate, and will take an infall-free (closed-box) model $f(t) = 0$ for the local ISM. The analytic solutions of these equations are easily generated if we take the star formation rate to be proportional to the mass of molecular clouds; $\psi(t) \equiv \omega_* M_{\rm MC}$. The simplified versions of equations (1) and (2) then read

$$\frac{dM_{\rm MC}}{dt} = -\omega_* M_{\rm MC} - \frac{M_{\rm MC}}{\tau} + \frac{M_{\rm DC}}{\tau}\,, \tag{3}$$

$$\frac{dM_{\rm DC}}{dt} = R\omega_* M_{\rm MC} - \frac{M_{\rm DC}}{\tau} + \frac{M_{\rm MC}}{\tau}\,, \tag{4}$$

which has one specific solution in which the masses of both phases decline at the same exponential rate, maintaining there-

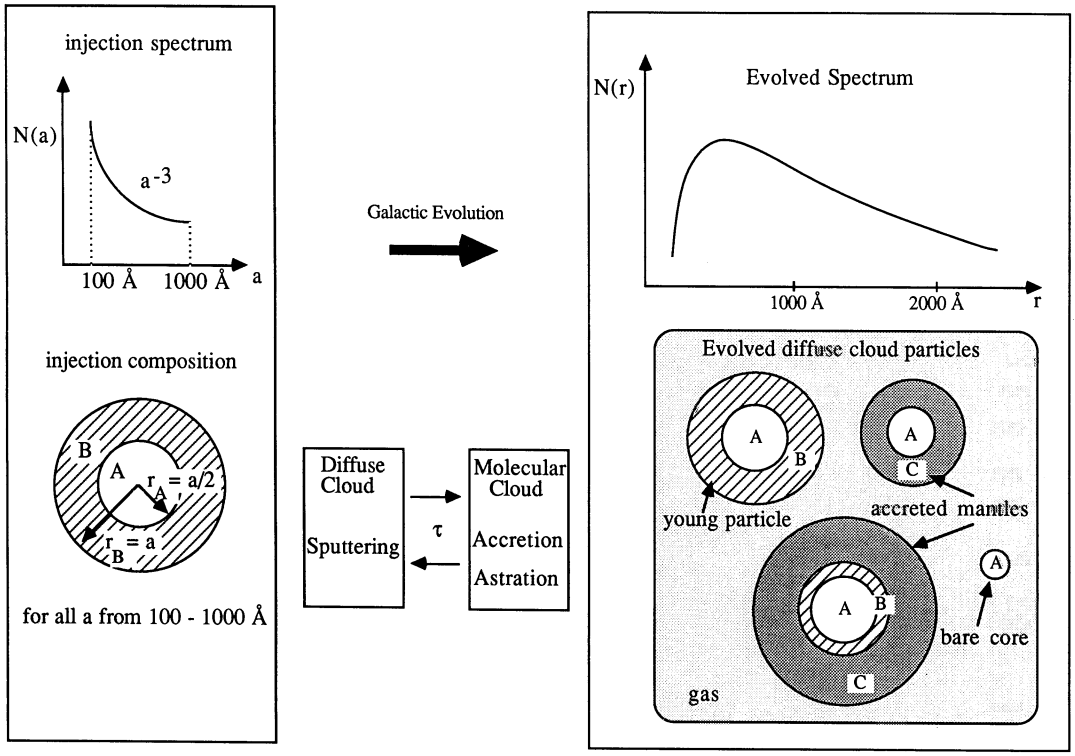

FIG. 1.—We assume that the dust grains are initially placed in the diffuse cloud phase and are created with an a^{-3} size spectrum (we are using the convention that the radius of a newly created dust grain is denoted by the symbol a) with a minimum and maximum size of 100 and 1000 Å respectively. Initially the dust grain consists of an inner core (labeled A) and an outer core-mantle (labeled B). These grains are injected continuously over time at an exponentially decreasing rate, and they reside for a mean time $\tau = 10^8$ yr in the different phases of the ISM. After a number of cycles between the diffuse and molecular media of the ISM, the grains' evolved size spectrum changes dramatically from the initial size spectrum (see Fig. 7 for a more exact representation), and the dust grains may have one of the cross sections as shown for the grains in the diffuse cloud: perhaps most or all of the B layer will have been eroded by sputtering and new layer (C) will have been formed by accretion of material during the particle's entries into the molecular clouds, or all of the mantles may have been eroded away by sputtering, leaving a bare core particle.

fore a constant ratio M_{MC}/M_{DC}, namely,

$$M_{DC} = M_{DC}(0)e^{\lambda_+ t}\,, \quad M_{MC} = M_{MC}(0)e^{\lambda_+ t} \tag{5}$$

and

$$M_{DC}(0)/M_{MC}(0) = -(1 + \tau\lambda_-)\,, \tag{6}$$

where

$$\lambda_\pm = -\left(\frac{1}{\tau} + \frac{\omega_*}{2}\right) \pm \left[\left(\frac{1}{\tau} + \frac{\omega_*}{2}\right)^2 - \frac{\omega_*}{\tau}(1 - R)\right]^{1/2}. \tag{7}$$

This particular solution reproduces, for the case of a two-phase medium, the exponential decline of gas that characterizes the familiar closed-box linear model (e.g., Clayton 1984). It goes over continuously to the one-phase ISM as the mixing time $\tau \to 0$, in which case equations (3), (4), and (6) yield $M_{DC} \to M_{MC}$ and $\lambda_+ \to -(1 - R)\omega_*/2$ and $\tau\lambda_- \to -2$. The value of λ_+ in this limit merits understanding. Because ω_* is the astration rate of the molecular medium, the astration rate of the combined media is just $\omega_*/2$, and the total gas consumption rate is reduced by the factor $(1 - R)$ owing to return from stars.

Because the primary purpose of this paper is to study the refractory dust component within a conventional framework for the chemical evolution of galaxies, we use equations (3)–(7) as exact descriptions of the total gas in a two-phase medium having the properties we have described for it. Even though the closed-box model is widely suspected of providing an inadequate description of the chemical evolution of the solar neighborhood (e.g., Tinsley 1980), we feel that this conventional simple model is appropriate for beginning considerations of the evolution of the dust, and, moreover, we believe that the properties to be calculated for the dust are not very sensitive to the criticisms that this model faces in matching galactic abundance data. In any case, we need a reliable analytic model for two reasons. The first is that exact solutions for abundances allow us a ready check of the accuracy of our numerical treatment. The second is that we also need and can generate the analogous exact solutions for the mass of refractory elements in each phase, $m_{DC} = Z_{DC} M_{DC}$ and $m_{MC} = Z_{MC} M_{MC}$, where Z is the interstellar mass fraction of the refractory element or elements under consideration. For primary nucleosynthesis products having a constant yield independent of stellar metallicity, these refractory-metal masses satisfy the equations (e.g., Tinsley 1980; Clayton 1984)

$$\frac{dm_{DC}}{dt} = y(1 - R)\Psi + Z_{MC} R\Psi - \frac{m_{DC}}{\tau} + \frac{m_{MC}}{\tau}\,, \tag{8}$$

$$\frac{dm_{MC}}{dt} = -Z_{MC}\Psi - \frac{m_{MC}}{\tau} + \frac{m_{DC}}{\tau}\,, \tag{9}$$

when cast into the two-phase form. Pay particular attention to the lowercase m here, distinguishing these metal masses from those in equations (1) and (2). For the linear star formation model $\psi = \omega_* M_{MC}$ we have solved these equations by using equation (5) for the star formation source term M_{MC}. These analytic solutions, which are very useful for checking the accuracy of our numerical treatment and seem not to have been previously presented, also provide an explicit rate for the injection of new refractory SUNOCONs (plus gas if any) into the ISM. The exact solutions for the bulk refractory-element masses are

$$m_{MC} = -\frac{y\omega_* M_{DC}(0)(1-R)}{\tau(1+\tau\lambda_-)(\lambda_+ - \lambda_-)} \times \left[t \exp(\lambda_+ t) + \frac{\exp(\lambda_- t) - \exp(\lambda_+ t)}{\lambda_+ - \lambda_-}\right], \quad (10)$$

$$m_{DC} = -\frac{y\omega_* M_{DC}(0)(1-R)}{(1+\tau\lambda_-)(\lambda_+ - \lambda_-)} \left\{\left(\lambda_+ + \frac{1}{\tau} + \omega_*\right) t \exp(\lambda_+ t) + \frac{\lambda_- + \omega_* + 1/\tau}{\lambda_+ - \lambda_-}[\exp(\lambda_- t) - \exp(\lambda_+ t)]\right\}. \quad (11)$$

For our numerical studies we have rather arbitrarily but not unreasonably chosen $\tau = 10^8$ yr (for mixing both ways), return fraction $R = \frac{1}{2}$, and astration rate within the molecular cloud $\omega_* = (1.5 \text{ Gyr})^{-1}$ corresponding to a mean astration time $\tau_{astr} \simeq 3$ Gyr for the combined media. With these choices $\lambda_+ = -0.1625$ Gyr^{-1} and $\lambda_- = -20.5041$ Gyr^{-1}, yielding $M_{MC}/M_{DC} = -(1 + \tau\lambda_-)^{-1} = 0.952$ for all t. From equations (10) and (11) we also obtain for large t the result that $m_{MC}/m_{DC} \to (\tau\lambda_+ + 1 + \tau\omega_*)^{-1} = 0.952$ asymptotically.

This analytic model of the closed-box chemical evolution of a two-phase ISM with interphase mixing provides the time dependence for the introduction of SUNOCONs into our numerical models of the dust evolution and also a check on the accuracy of several numerical quantities. From the first term of equation (8) the rate of injection of new refractory metals is

$$\left(\frac{dm_{DC}}{dt}\right)_+^{new} = y(1-R)\psi = y(1-R)\omega_* M_{MC} = \frac{1}{2} y\omega_* M_{MC}(0) \exp(\lambda_+ t), \quad (12)$$

which declines exponentially with time scale $(|\lambda_+|)^{-1} = 6.15$ Gyr if $R = \frac{1}{2}$. Having decided what fraction of these new metals condense within SUNOCONs (100% or 50% in the cases to be reported), we inject those SUNOCONs into our diffuse medium at the rate given by equation (12). From equations (12) and (6), one can obtain the integrated mass of new refractory material ever ejected from stars:

$$\sum^{new}(t) \equiv \int_0^t \left(\frac{dm_{DC}}{dt}\right)_+^{new} dt = \frac{y\omega_*(1-R)M_{DC}(0)}{\lambda_+(1+\tau\lambda_-)}\left[1 - \exp(\lambda_+ t)\right]. \quad (13)$$

The second term of equation (8) gives the rate of refractory-element return from stars

$$\left(\frac{dm_{DC}}{dt}\right)_+^{old} = Z_{MC} R\psi = \omega_* R Z_{MC} M_{MC} = \frac{1}{2}\omega_* m_{MC}, \quad (14)$$

where m_{MC} is given exactly by equation (11) and $R = \frac{1}{2}$ in the last quantity. We need only specify whether the return is gaseous or STARDUST. Thus the integrated mass of old refractory material ever returned from stars is

$$\sum^{old}(t) = \int_0^t \left(\frac{dm_{DC}}{dt}\right)_+^{old} dt = -\frac{y\omega_*^2 R(1-R)M_{DC}(0)}{\tau(1+\tau\lambda_-)(\lambda_+ - \lambda_-)} \times \left\{\frac{t\exp(\lambda_+ t)}{\lambda_+} + \frac{\exp(\lambda_- t) - 1}{\lambda_-(\lambda_+ - \lambda_-)} - \frac{2\lambda_+ - \lambda_-}{\lambda_+^2(\lambda_+ - \lambda_-)} \times [\exp(\lambda_+ t) - 1]\right\}. \quad (15)$$

As $t \to \infty$,

$$\frac{\sum^{old}}{\sum^{new}} \to \frac{R}{1-R} = 1 \quad \text{for } R = \frac{1}{2}. \quad (16)$$

This last limit can be readily understood by following the evolution of a unit mass of newly created refractory material. After a suitably long time, this material will be incorporated into stars via the process of astration, and a fraction R of it will be returned to the ISM. This fraction of material will in turn be astrated, and again a fraction R of it will be returned. As time becomes very large, the ratio of the total sum of reinjected material to the unit mass of initial refractory material is

$$\frac{R + R^2 + R^3 + \cdots}{1} = \frac{R}{1-R} \quad (0 < R < 1). \quad (17)$$

III. EVOLUTION OF THE REFRACTORY DUST

As mentioned in § I, we inject all newly created particles, whether they be SUNOCONs or STARDUST, into the diffuse medium along with whatever gaseous atoms are ejected from the stars. These new dust grains are given a truncated power-law size spectrum of $n(a)da = Ka^{-3}da$, 100 Å $\leq a \leq$ 1000 Å (where a is the initial radius of the dust grain and K is an arbitrary constant which is dependent on the total number of dust grains injected into the ISM), which is suggested by the grain-size spectra deduced from extinction studies (Mathis 1985). To obtain a better understanding of our model interstellar medium, we consider the three aforementioned cases. For the sake of clarity, we present in Table 1 the physical characteristics of each case.

a) Sputtering

While the dust grains are resident in the diffuse medium, they are subject to the erosive process of sputtering. If we assume that our dust grains are spherical, then the rate of mass loss is

$$\frac{dM_{grain}}{dt} = -K\sigma, \quad (18)$$

TABLE 1

CASES FOR CONDENSATION DURING INJECTION

Injecta	Case 1	Case 2	Case 3
SUNOCONs	100% solid	50% solid	100% solid
STARDUST	100% gaseous	100% gaseous	100% solid
Sputtering	Thermal	Thermal	Thermal

where M_{grain} is the mass of the grain, σ is the surface area of the grain, and K is the mass yield per unit area per unit time. Thus

$$\frac{dr}{dt} = -\frac{K}{\rho}, \qquad (19)$$

r being the radius of the dust grain at time t. In the results presented here, we consider only thermal sputtering (i.e. the dust grains are immersed in a hot postshock Mawellian gas), even though inertial sputtering following acceleration by the shock waves may be a major source of dust grain erosion (Shull 1978; Draine and Salpeter 1979*a*, *b*; Seab and Shull 1983; Tielens *et al.* 1987). Our initial study (Liffman and Clayton 1988) also simulated inertial sputtering in an approximate manner. The effect of such sputtering was contrasted to that of thermal sputtering and will be discussed in § IV. For purposes of constructing a chemical evolution model, however, thermal sputtering will be sufficient. We envision a radial sputtering erosion rate in the diffuse medium that is constant with time, even though it is really a series of reheating events as shock waves propagate through the diffuse medium. We have taken $K/\rho = 0.02\ \mu\text{m}/10^8$ yr, which is consistent with a mass lifetime of approximately 2×10^8 years for a 0.1 μm dust grain.

Sputtering actually occurs in all interstellar phases—in diffuse clouds, in the intercloud warm gas, and in molecular clouds whenever an embedded supernova produces a shock wave that propagates into the molecular cloud as well as into the warmer gas that has already been created by the starburst disruption of the molecular cloud. Essentially we ignore the molecular cloud sputtering on two grounds: (1) we believe it to be small in the overall rate of sputtering; (2) if the medium remains molecular, the sputtered atoms are quickly reaccreted, with little net effect. If the supernova shock disrupts the molecular medium, on the other hand, we regard the associated sputtering as the first (of many) recurrent episodes of sputtering that will contribute to the net sputtering of this dust while it resides in its new diffuse gas state. The substantial sputtering that occurs in the warm intercloud gas, on the other hand, is regarded by us as being one mode of sputtering of the diffuse medium. We imagine that this low-mass intercloud gas is incorporated into diffuse clouds much faster than the diffuse clouds are disrupted, thereby accounting for the smallness of this intercloud mass, which we have simply suppressed in our simplification to a two-phase medium.

b) Accretion

When a dust grain transfers as a part of a transit cloud from the diffuse medium to a molecular cloud, it accretes a mantle of thickness Δr. The rate at which the radius of a spherical dust grain accretes this mantle is

$$\frac{dr}{dt} = \frac{mn\langle v\rangle\alpha}{4\rho_g}, \qquad (20)$$

where m is the mass of a condensable gas atom, n is the condensable gas number density, $\langle v\rangle$ is the mean thermal speed of the refractory gas atoms relative to the dust grain in the rapidly chilling transit cloud, α is the probability of an incident particle sticking to a dust grain, and ρ_g is the density of the dust grain. If the dust grains are all in the same physical environment, then the rate of grain growth will be the same for all dust grains. Thus all the dust grains will obtain the same thickness of accreted material (Δr) irrespective of the initial size of the dust grain as it enters the molecular cloud (Clayton 1980). This simple but significant result, plus the assumption that the transit cloud is a sample of a uniform well-mixed diffuse medium, allows us to derive (see the Appendix) a cubic equation which gives the thickness of the accreted mantle in terms of readily computable quantities:

$$(\Delta r)^3 + 3(\Delta r)^2\langle r\rangle_{DC} + 3\Delta r\langle r^2\rangle_{DC} - \frac{3M}{4\pi k\rho_g} = 0\,, \qquad (21)$$

where $\langle r\rangle_{DC}$ is the average radius of the dust grains in the diffuse medium, $\langle r^2\rangle_{DC}$ is the average square of the radius of the dust grains in the diffuse medium, M is the mass of condensable material in the diffuse medium, and k is the number of dust particles in the diffuse medium. We call this equation the "accretion equation," and it is the fundamental connection between the gaseous and solid phase of our model ISM. The final term, $3M/4\pi k\rho_g$, represents the total volume of material per dust grain that is available for accretion. The assumption of uniformity owing to mixing is crucial to many of our results, innocuous though it may seem, because if each transit cloud reaccreted only those atoms that had been previously sputtered away from its dust grains, no migration in dust grain size would occur. Our Monte Carlo treatment assumes that the increment of mantle thickness accreted by each dust grain is independent of its history and that of its neighbors. By the same token we omit in this study any gas/dust fractionation that may in reality occur in real diffuse clouds; but we have confirmed by trial calculations that a stochastic spread in Δr about a mean leads to no great change in our results.

c) Data Handling and Stochastic Transfers

In this section we describe the form of our Monte Carlo program. We construct a description of an evolving dust ecology based on studying the individual physical behavior of each dust grain in a large collection of such grains. Our aim is to obtain the mass spectrum, size spectrum, and distribution of internal structure of the evolved dust population. This is done by creating and placing a finite number of dust grains into a memory matrix at each time step, where each dust grain occupies one row of that matrix.

For example, at $t = 0$ we place n_0 (say) dust particles into the matrix (remembering that particles are initially injected into the diffuse medium). At $t = \Delta t$ we place n_1 more dust particles into the matrix, and we calculate the fraction of the earlier dust grains that have been transferred to the molecular cloud phase or have been destroyed by sputtering. For those particles remaining in the diffuse phase, we record the changes in their structure owing to the sputtering. This process continues in the same way for subsequent time steps, so that at

$t = 2\Delta t$ we place n_2 dust grains into the matrix ,

.

.

.

$t = m\Delta t$ we place n_m dust grains into the matrix .

The relationship between the n_j is easily derived from equation (12). If we take the number of injected dust particles per time step to be proportional to the mass of refractory material injected into the medium per time step, we then write

$$\Delta N = N_0 \exp(\lambda_+ t)\Delta t\,, \qquad (22)$$

where N_0 is a constant normalizing the absolute rate of particle injection. The number injected during time step j is then

$$n_j = N_0 \exp(\lambda_+ j\Delta t)\Delta t \ . \quad (23)$$

The probabilities for particle transfer to a different phase and for astration in the molecular clouds are both given by the basic Monte Carlo equation:

$$\int_a^t p(t)dt = G \ , \quad a < t < b \ , \quad (24)$$

where G is a random number, and in our case

$$p(t)dt = \exp\left(-\frac{t}{\tau}\right)\frac{dt}{\tau} \quad (25)$$

is the probability that a particle remains in the same phase for a duration t before being transferred during the interval dt. So the probability for a dust particle to transfer to a different interstellar phase in the time interval 0 to t is $1 - \exp(-t/\tau)$, where $\tau = 10^8$ yr. Our procedure is to generate a random number G for each particle and for each time step Δt (G being the uniform distribution on the closed interval [0, 1]), and if $G < 1 - \exp(-\Delta t/\tau)$, then the particle transfers to the other interstellar phase. We handle the astration of particles in a similar fashion, except that $\tau = 1.5 \times 10^9$ yr.

We process all the dust particles at one time, and because we calculate explicitly the mass of refractory gas maintained in the diffuse medium, it is possible to compute Δr—the thickness of the accreted mantle—as a function of time. This is accomplished by using equation (21) (see also the next subsection and Fig. 5). The final term in this equation contains the quotient M/k, where M is the total mass of condensable gas within a physical subcloud of well-mixed gas and dust being transferred from the diffuse cloud to the molecular cloud and k is the number of dust grains in that transit cloud. Although M/k refers to this transit cloud, for statistical purposes we take it to be equal to the same ratio for the corresponding material in the entire diffuse medium. Thus k is easily determined as the total number of dust grains in the diffuse medium. The calculation of M—the total mass of condensable refractory gas atoms in the diffuse medium— is slightly more complicated, for as we move down the rows of the particle matrix and process each dust grain in turn, we must consider the following:

1. *Is the particle in the diffuse medium?* If yes, the particle is sputtered for a time step of Δt and the liberated mass of refractory atoms is added to M.
2. *Is the particle being transferred from the diffuse medium to the molecular cloud phase?* If so, the particle will accrete material and so reduce M by the mass of refractory material accreted.
3. *Is the particle astrated in the molecular cloud phase?* If so, half of all the material astrated will—by our construction—be returned to the diffuse medium as gas or as new STARDUST. At most half (totally gaseous return) the mass of the dust particle must be added to M, but only at the start of the next time step, since the particle has been astrated during the time step.

With these logical instructions in place along with the sputtering description of equation (19), we obtain single-particle histories producing population profiles similar to those shown in Figure 1. The collective evolution is discussed in the following sections.

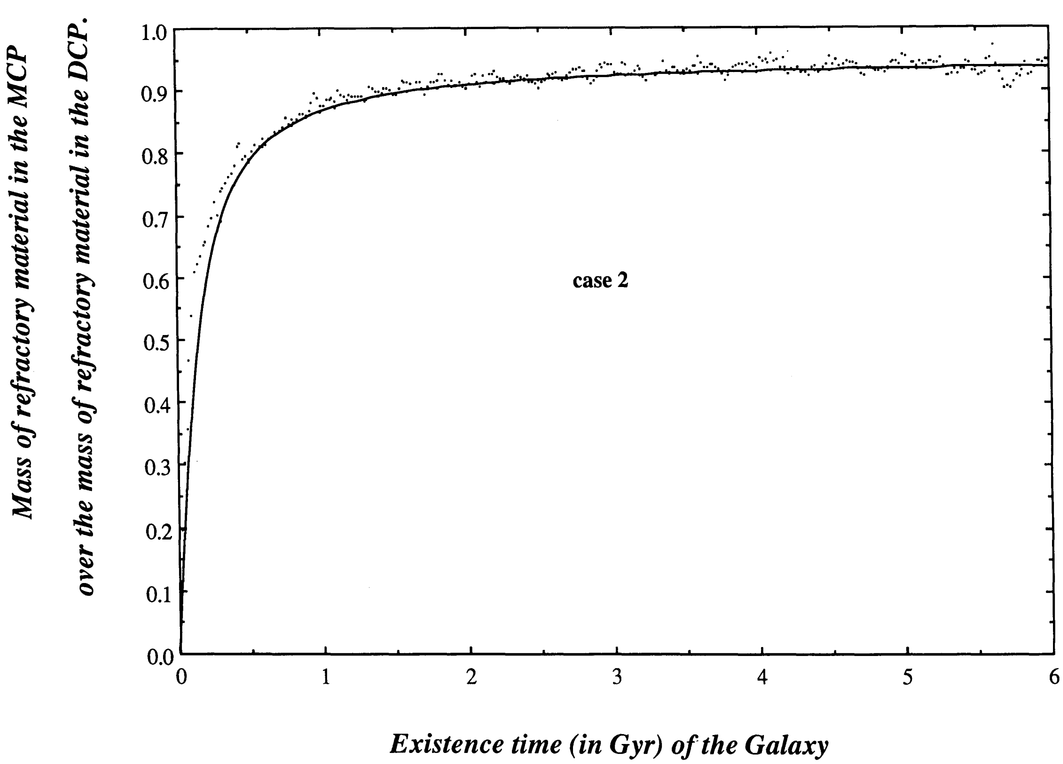

FIG. 2.—Ratio of the mass of refractory material in the molecular cloud medium to the mass of refractory material in the diffuse medium, as a function of time, for case 2. The solid line represents the analytic solution as given by the ratios of eqs. (10) and (11), while the scattered points represent points from the Monte Carlo solution.

d) Comparisons of Calculated Masses with Their Analytic Representations

A major concern in any numerical simulation is the question of accuracy. We partially address such concern and study the evolution of our system by comparing the analytic results obtained in § II with the results garnered from our Monte Carlo simulations.

Figure 2 shows such a comparison. Here we have the mass ratio of the refractory material in the molecular clouds to the mass of such material in the diffuse medium as a function of time. The simulation results generally follow the analytic solution (the ratio of eqs. [10] and [11]) toward an asymptotic value of 0.952. However, the simulation mass ratio of the two phases shows considerable fluctuation relative to the analytic solution. This is due to the negative feedback produced from the formation of an accretion mantle as particles are transferred from the diffuse cloud phase to the molecular cloud phase. This process may be most clearly seen by comparing Figures 2 and 5*b*.

In case 2 there is initially no refractory mass in the molecular cloud, and 50% of the refractory mass in the diffuse medium is available for accretion onto the transferring dust grains. Thus Δr (the thickness of the accreted mantle) takes on a large initial value, and a significant proportion of the total refractory mass is quickly transferred to the molecular cloud phase. The barely visible initial divergence between the analytic and numerical solutions in Figure 2 shows that too much mass is being transferred to the molecular cloud phase. This causes a "shortage" of condensable refractory gas in the diffuse medium, and Δr decreases accordingly (see Fig. 5*b*). The remaining fluctuations in the mass ratio correlate inversely with Δr, i.e., when the mass ratio is too high, Δr decreases and vice versa. The aforementioned initial divergence between the analytic and numerical solutions in Figure 2 is a consequence of a noninfinitesimal time step of 10^7 yr in our Monte Carlo simulation and of our procedure of transferring masses at the end of each time step. One should note that this and all other simulations presented here are taken to times of 6 Gyr, because the Galaxy was probably at least that old when the solar system first formed.

Two similar calculations are shown in Figures 3 and 4. In Figure 3 we plot (again for the case 2 example; 50% SUNOCON condensation, but totally gaseous return) the mass of refractory atoms in the ISM $[m_{\rm DC}(t) + m_{\rm MC}(t)]$ over the total mass of new refractories ever placed in the ISM $[\sum^{\rm new}(t)]$. The ratio $[m_{\rm DC}(t) + m_{\rm MC}(t)]/\sum^{\rm new}(t)$ is seen to decrease with time. It does so because refractory material is continually consumed via astration and is only partially returned ($R = \frac{1}{2}$). The fluctuations are much smaller in Figure 3 than in Figure 2, because they are due to the statistical fluctuations in the mass astrated, which is small compared with the combined refractory mass of the two ISM phases. In Figure 4 we plot for case 3 the ratio of the integrated injection of old and new matter, $\sum^{\rm old}(t)/\sum^{\rm new}(t)$, which increases from its initial value of zero toward the asymptotic ratio $R/(1 - R) = 1$ (this value is not reached in 6 Gyr). The numerical results in all cases examined are close to the analytic results, which do not depend on the case chosen, and the observed fluctuations are reasonable for numerical simulation. This agreement provides us with confidence in those subsequent results which are not obtainable via analytic means and which are the main objectives in this study.

e) Accreted Mantle Thickness

The thickness of the accreted mantle is determined by the amount of condensable material available per dust grain as the transit cloud transmutes from the diffuse medium phase to the molecular cloud phase. We should expect that Δr for cases 1 and 3 will initially be of zero length, since all the refractories are injected as solid grains and it will take a certain amount of sputtering before enough refractory gas is present in the diffuse medium to accrete back onto the dust grains. Contrasting behavior should occur for case 2, because 50% of the new refractories are injected into the diffuse medium as gas in that case. Our expectations are realized in Figures 5*a* and 5*b*. In both figures we have an initial transitory epoch of less than 500 Myr duration, during which the system comes into a steady state of mass balance between the molecular and diffuse media. For times greater than 500 Myr, Δr increases at a steady rate.

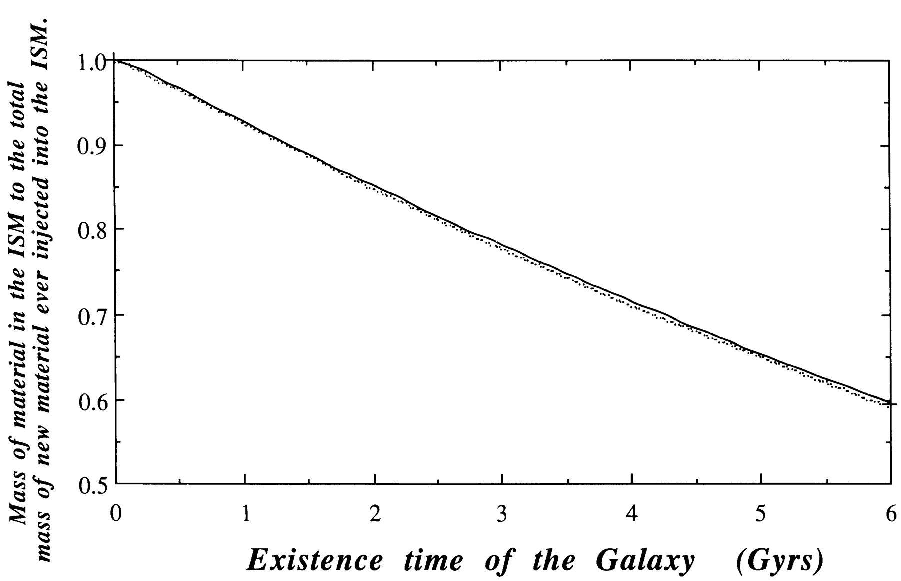

FIG. 3.—Ratio of the mass of material in the ISM to the total mass of new material ever injected into the ISM for the analytic solution (*solid line*) and the case 2 Monte Carlo solution (*dots*), as a function of time. The ratio decreases with time, because material is taken out of the ISM via the process of astration.

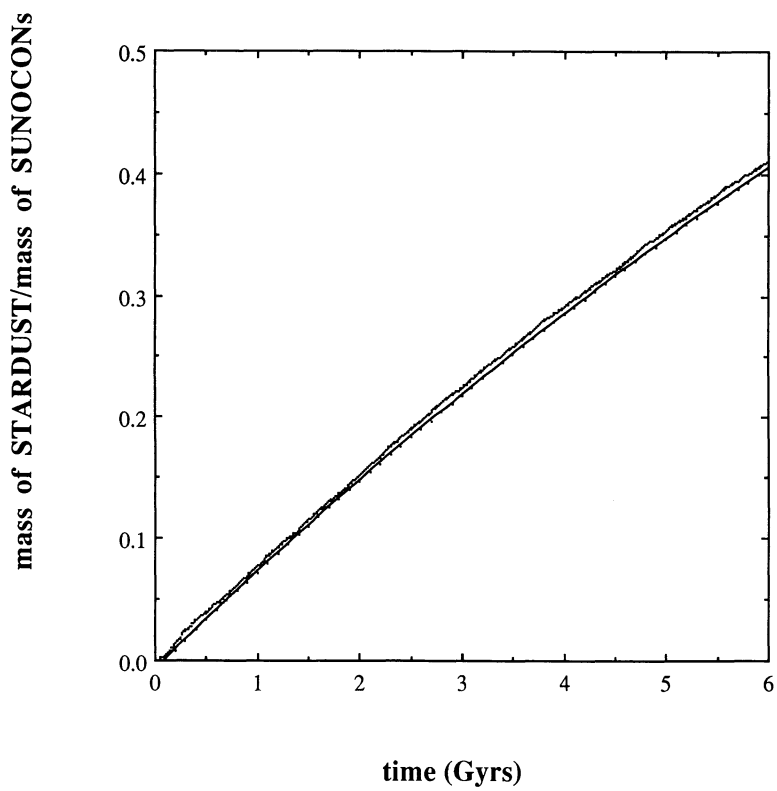

FIG. 4.—Ratio of the total mass of refractory atoms (STARDUST plus gas) ever returned from stars to the total mass of new refractory atoms (SUNOCONs plus gas) injected into the interstellar medium, as a function of time, for case 3. If the simulation is continued for a long enough time, then the two lines should reach an asymptotic value $R/(1 - R)$, which is unity for our choice of $R = \frac{1}{2}$.

This result is not really surprising, since the dust grains are being destroyed on time scales of 3×10^8 to 10^9 yr and the gas can only be destroyed on the time scale of star formation: 3×10^9 yr. Thus one should expect the amount of gas per grain to increase with time. Grains that have been destroyed do not reappear as entities, but their mass must be added to that of other grains, so Δr must increase.

A side benefit of modeling the interstellar dust system in this manner is our ability to monitor the amount of refractory gas in the diffuse medium. We know from observations of the ISM that elements such as aluminum and magnesium are severely depleted in the gas phase relative to cosmic abundances. The inference is that most of these elements are contained in the dust grains. The results of Figure 6 show immediately that our current interstellar model does not give the expected depletions, because at $t = 6$ Gyr over 50% of the refractory mass in the diffuse cloud is gaseous, while observations suggest that less than 1% of all interstellar aluminum and magnesium is

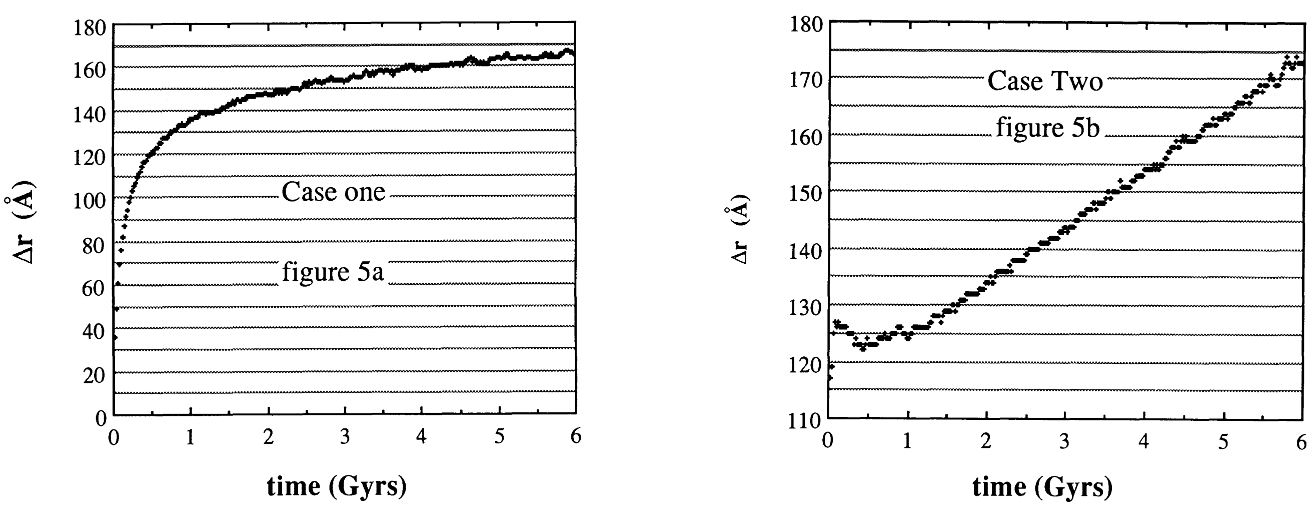

FIG. 5.—Thickness of the accreted mantle as a function of time for (*a*) case 1 and (*b*) case 2. The behavior of case 3 is similar to that of case 1, except that Δr only goes to 150 Å.

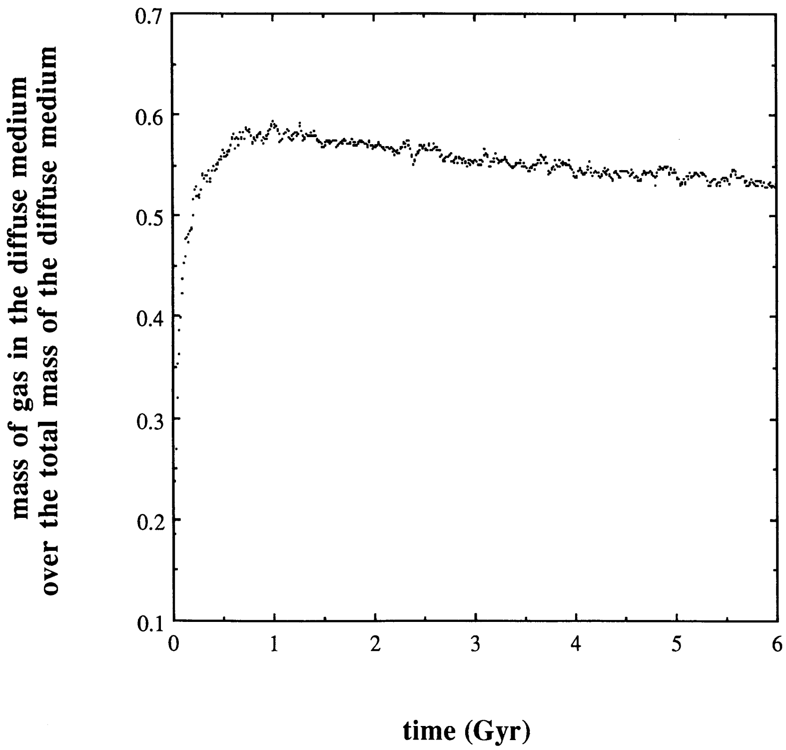

FIG. 6.—A typical example of the ratio of the mass of condensable gas in the diffuse medium to the total condensable mass of the diffuse medium, as a function of time, for case 3. As can be seen, refractory material is not significantly depleted in the diffuse phase.

found in the gas phase. We will return to this discrepancy in the next section.

IV. DISCUSSION

At the age of 6 Gyr we examine in detail the physical and chemical structure of the interstellar dust system. In Tables 2–4 we present the data obtained for each of the cases considered, and in the following subsections we discuss the size spectrum, depletions, lifetimes, and anomalous isotopic composition of the dust particles. One should note that in the tables the first column describes the quantities being tabulated, with the convention that physical units are contained in parentheses whereas abbreviations are shown in braces. Most of the terms are self-explanatory, but for the sake of clarity we note that the core and core-mantle as referred to in lines 30 and 39 of Table 2 are just the A and B sections, respectively, of our dust particles (see Fig. 1). Table 4 breaks down the dust population into those with SUNOCON cores and those with STARDUST cores.

a) Size Spectrum

Figure 7 displays both the injected and the evolved dust size spectra for case 2, i.e., 50% SUNOCON condensation, but gaseous return. The major differences between the two spectra are (1) the large decrease of particles with sizes around 100 Å and (2) the change from an a^{-3} injected distribution to a exponential-like evolved size spectrum.

It is possible to understand this result if we consider the processes occurring on the dust particles. As the particles oscillate between the different interstellar media, they are reduced in size via sputtering and increased in size by accretion. We can think of this as a random walk in size with the added feature that the particles can be destroyed if sputtering decreases their size down to molecular dimensions, which we take to be 5 Å. This feature renders the problem analogous to the one of a random walk with an absorbing wall (Chandrasekhar 1943), the integrated solution to which is of exponential form.

The difference at small radii between the computed size spectrum and the observationally inferred size spectra (Mathis, Rumpl, and Nordsieck 1977; Greenberg 1978; Rowan-Robinson 1986) suggests that some other ingredient is required in our model. The maintenance of a large population of small particles may be achieved by the inclusion of grain-grain fragmentation. Preliminary results of such a model (Liffman 1988) suggest that the dust size spectrum evolves under fragmentation into a bimodal distribution consisting of small bare grains and large mantled grains. The results from this and other studies will be presented at a later date.

The work of Liffman and Clayton (1988) has shown that if one considers an alternative sputtering prescription based on inertial sputtering, then the evolved size spectrum is a truncated version of that shown in Figure 7. This is due to the fact that intertial sputtering is proportional to radius and so larger particles are eroded more rapidly than smaller particles. We have confirmed this contrasting behavior, which Liffman and Clayton (1988) generated from single-particle histories, with the Galactic evolution approach of this work. We will not display these results, however, because the contrast conveys no more information than already obtained in our earlier work.

b) Depletions

A major reason for calculating explicitly the mass balance of refractory atoms in the diffuse medium is the attempt to under-

TABLE 2

GRAIN POPULATION CHARACTERISTICS FOR CASE 1

Quantity	Value
1. Number of particles injected, $\{N_i\}$	1,534,029
2. Maximum size increment due to accretion $\{\Delta r\}$ (Å)	165
3. Number destroyed in the diffuse cloud $\{N_{d\,\mathrm{DC}}\}$	1,255,783
4. Number destroyed in the molecular cloud $\{N_{d\,\mathrm{MC}}\}$	195,443
5. Number surviving in the diffuse cloud $\{N_{s\,\mathrm{DC}}\}$	41,780
6. Number surviving in the molecular cloud $\{N_{s\,\mathrm{MC}}\}$	41,022
7. Total number surviving $\{N_f\}$	82,802
8. N_f/N_i (%)	5.40%
9. $N_{s\,\mathrm{DC}}/N_{s\,\mathrm{MC}}$	1.018
10. Total grain mass injected $\{M_{\mathrm{injected}}\}$ (kg)	1.17×10^{-13}
11. Total grain mass sputtered $\{M_{\mathrm{sputter}}\}$ (kg)	7.79×10^{-13}
12. Total grain mass astrated $\{M_{\mathrm{astrated}}\}$ (kg)	9.63×10^{-14}
13. Total mass accreted $\{M_{\mathrm{accreted}}\}$ (kg)	8.09×10^{-13}
14. Total surviving grain mass $\{M_{\mathrm{grain\,final}}\}$ (kg)	5.10×10^{-14}
15. Total final gas mass $\{M_{\mathrm{gas}}\}$ (kg)	1.80×10^{-14}
16. Total mass $\{M_{\mathrm{final}}\}$ (kg)	6.90×10^{-14}
17. $M_{\mathrm{final}}/M_{\mathrm{injected}}$	0.59
18. Total grain mass in the diffuse cloud $\{M_{\mathrm{grain\,DC}}\}$ (kg)	1.734×10^{-14}
19. Total grain mass in the molecular cloud $\{M_{\mathrm{grain\,MC}}\}$ (kg)	3.369×10^{-14}
20. $M_{\mathrm{gas}}/(M_{\mathrm{grain\,DC}} + M_{\mathrm{gas}})$	51%
21. M_{final}/N_f (kg)	8.33×10^{-19}
22. $M_{\mathrm{injected}}/N_i$ (kg)	7.64×10^{-20}
23. $M_{\mathrm{sputter}}/M_{\mathrm{accreted}}$	0.96
24. $M_{\mathrm{sputter}}/M_{\mathrm{final}}$	11.29
25. $M_{\mathrm{astrated}}/M_{\mathrm{final}}$	1.40
26. $M_{\mathrm{accreted}}/M_{\mathrm{final}}$	11.73
27. $M_{\mathrm{sputter}}/M_{\mathrm{injected}}$	6.65
28. $M_{\mathrm{astrated}}/M_{\mathrm{injected}}$	0.82
29. $M_{\mathrm{accreted}}/M_{\mathrm{injected}}$	6.91
30. Total mass of core injected $\{M_{\mathrm{A.injected}}\}$ (kg)	1.47×10^{-14}
31. Total mass of core sputtered $\{M_{\mathrm{A.sputter}}\}$ (kg)	9.96×10^{-15}
32. Total mass of core astrated $\{M_{\mathrm{A.astrated}}\}$ (kg)	3.25×10^{-15}
33. Total mass of core surviving $\{M_{\mathrm{A.final}}\}$ (kg)	1.44×10^{-15}
34. $M_{\mathrm{A.final}}/M_{\mathrm{A.injected}}$ (%)	9.83%
35. $M_{\mathrm{A.sputter}}/M_{\mathrm{A.injected}}$ (%)	67.97%
36. $M_{\mathrm{A.astrated}}/M_{\mathrm{A.injected}}$ (%)	22.20%
37. $M_{\mathrm{A.final}}/M_{\mathrm{final}}$ (%)	2.09%
38. $M_{\mathrm{A.injected}}/M_{\mathrm{injected}}$ (%)	12.50%
39. Total mass of core-mantle injected $\{M_{\mathrm{B.injected}}\}$ (kg)	1.03×10^{-13}
40. Total mass of core-mantle sputtered $\{M_{\mathrm{B.sputter}}\}$ (kg)	9.04×10^{-13}
41. Total mass of core-mantle astrated $\{M_{\mathrm{B.astrated}}\}$ (kg)	8.59×10^{-15}
42. Total mass of core-mantle surviving $\{M_{\mathrm{B.final}}\}$ (kg)	3.54×10^{-15}
43. $M_{\mathrm{B.final}}/M_{\mathrm{B.injected}}$ (%)	3.45%
44. $M_{\mathrm{B.sputter}}/M_{\mathrm{B.injected}}$ (%)	88.17%
45. $M_{\mathrm{B.astrated}}/M_{\mathrm{B.injected}}$ (%)	8.38%
46. $M_{\mathrm{B.final}}/M_{\mathrm{final}}$ (%)	5.13%
47. $M_{\mathrm{B.injected}}/M_{\mathrm{injected}}$ (%)	87.50%
48. $M_{\mathrm{B.injected}}/M_{\mathrm{A.injected}}$	7.00
49. $M_{\mathrm{B.final}}/M_{\mathrm{A.final}}$	2.46

stand the observed depletions of elements in the diffuse clouds. Elements like magnesium and aluminum are depleted relative to solar abundances by factors of around 100 and 1000, respectively (Salpeter 1977; Cowie and Songaila 1986). We have tried to obtain these depletions by assuming that the dust grains are preferentially layered owing to sequential thermal condensation during the ejection from stars. The more refractory material in such a sequence falls naturally at the centers of the grains. Differential depletions are then established, because the erosive process of the ISM must first erode away the less refractory material (Clayton 1982). This approach elaborates the work of Field (1974), who noted that there was a correlation between depletions and condensation temperature of the elements.

The results that we have obtained do not yield the observed depletions. In Figure 6 and in line 22 of Table 4 we see that, for this model, 53% by mass of all the refractory material in the diffuse media is in the gaseous state, a result that is in stark contrast to the observationally observed 1% for aluminum and magnesium. One should note, however, that elements such as carbon, nitrogen, sulfur, and oxygen have depletion ratios (i.e., the ratio of abundance in the gas to cosmic abundance) that begin to approach the depletions shown in Figure 6. From the information in the tables, we can also obtain some idea of the relative depletions of aluminum and magnesium in our ISM. Their differential depletion is an objective of the core-mantle model.

Our astrophysical model is perhaps too crude to expect better success with the absolute and differential depletions. By concentrating on the major refractory elements (here envisioned as Mg, Si, Al, Ca, Fe, and their oxides), we have neglected the role of carbonaceous mantles. Carbon mass is

TABLE 3

GRAIN POPULATION CHARACTERISTICS FOR CASE 2

Quantity	Value
1. Number of particles injected $\{N_i\}$	1,260,321
2. Maximum size increment due to accretion $\{\Delta r\}$ (Å)	178
3. Number destroyed in the diffuse cloud $\{N_{d\,\mathrm{DC}}\}$	982,805
4. Number destroyed in the molecular cloud $\{N_{d\,\mathrm{MC}}\}$	185,744
5. Number surviving in the diffuse cloud $\{N_{s\,\mathrm{DC}}\}$	46,518
6. Number surviving in the molecular cloud $\{N_{s\,\mathrm{MC}}\}$	45,254
7. Total number surviving $\{N_f\}$	91,772
8. N_f/N_i (%)	7.28%
9. $N_{s\,\mathrm{DC}}/N_{s\,\mathrm{MC}}$	1.028
10. Total grain mass injected $\{M_{\mathrm{grain\,injected}}\}$ (kg)	9.62×10^{-14}
11. Total mass injected $\{M_{\mathrm{injected}}\}$ (kg)	1.92×10^{-13}
12. Total grain mass sputtered $\{M_{\mathrm{sputter}}\}$ (kg)	1.09×10^{-12}
13. Total grain mass astrated $\{M_{\mathrm{astrated}}\}$ (kg)	1.51×10^{-13}
14. Total mass accreted $\{M_{\mathrm{accreted}}\}$ (kg)	1.23×10^{-12}
15. Total surviving grain mass $\{M_{\mathrm{grain\,final}}\}$ (kg)	8.81×10^{-14}
16. Total final gas mass $\{M_{\mathrm{gas}}\}$ (kg)	2.89×10^{-14}
17. Total mass $\{M_{\mathrm{final}}\}$ (kg)	1.17×10^{-13}
18. $M_{\mathrm{final}}/M_{\mathrm{injected}}$	0.61
19. Total grain mass in the diffuse cloud $\{M_{\mathrm{grain\,DC}}\}$ (kg)	3.19×10^{-14}
20. Total grain mass in the molecular cloud $\{M_{\mathrm{grain\,MC}}\}$ (kg)	5.16×10^{-14}
21. $M_{\mathrm{gas}}/(M_{\mathrm{grain\,DC}} + M_{\mathrm{gas}})$	47%
22. M_{final}/N_f (kg)	1.27×10^{-18}
23. $M_{\mathrm{injected}}/N_i$ (kg)	7.63×10^{-20}
24. $M_{\mathrm{sputter}}/M_{\mathrm{accreted}}$	0.88
25. $M_{\mathrm{sputter}}/M_{\mathrm{final}}$	9.29
26. $M_{\mathrm{astrated}}/M_{\mathrm{final}}$	1.29
27. $M_{\mathrm{accretion}}/M_{\mathrm{final}}$	10.50
28. $M_{\mathrm{sputter}}/M_{\mathrm{injected}}$	11.30
29. $M_{\mathrm{astrated}}/M_{\mathrm{injected}}$	1.57
30. $M_{\mathrm{accreted}}/M_{\mathrm{injected}}$	12.78
31. Total mass of core injected $\{M_{\mathrm{A.injected}}\}$ (kg)	1.20×10^{-14}
32. Total mass of core sputtered $\{M_{\mathrm{A.sputter}}\}$ (kg)	7.48×10^{-15}
33. Total mass of core astrated $\{M_{\mathrm{A.astrated}}\}$ (kg)	2.97×10^{-15}
34. Total mass of core surviving $\{M_{\mathrm{A.final}}\}$ (kg)	1.57×10^{-15}
35. $M_{\mathrm{A.final}}/M_{\mathrm{A.injected}}$ (%)	13.07%
36. $M_{\mathrm{A.sputter}}/M_{\mathrm{A.injected}}$ (%)	62.25%
37. $M_{\mathrm{A.astrated}}/M_{\mathrm{A.injected}}$ (%)	24.68%
38. $M_{\mathrm{A.final}}/M_{\mathrm{final}}$ (%)	1.34%
39. $M_{\mathrm{A.injected}}/M_{\mathrm{injected}}$ (%)	12.50
40. Total mass of core-mantle injected $\{M_{\mathrm{B.injected}}\}$ (kg)	8.41×10^{-14}
41. Total mass of core-mantle sputtered $\{M_{\mathrm{B.sputter}}\}$ (kg)	7.21×10^{-14}
42. Total mass of core-mantle astrated $\{M_{\mathrm{B.astrated}}\}$ (kg)	8.03×10^{-15}
43. Total mass of core-mantle surviving $\{M_{\mathrm{B.final}}\}$ (kg)	4.02×10^{-15}
44. $M_{\mathrm{B.final}}/M_{\mathrm{B.injected}}$ (%)	4.78%
45. $M_{\mathrm{B.sputter}}/M_{\mathrm{B.injected}}$ (%)	85.68%
46. $M_{\mathrm{B.astrated}}/M_{\mathrm{B.injected}}$ (%)	9.54%
47. $M_{\mathrm{B.final}}/M_{\mathrm{final}}$ (%)	3.44%
48. $M_{\mathrm{B.injected}}/M_{\mathrm{injected}}$ (%)	87.50%
49. $M_{\mathrm{B.injected}}/M_{\mathrm{A.injected}}$	7.00
50. $M_{\mathrm{B.final}}/M_{\mathrm{A.final}}$	2.56

considerably greater than the mass of the metals we have considered. If a large carbon mantle shields the other refractory elements, the need of first sputtering it away would increase the absolute depletions of the refractory cores, which we have seen fail by an order of magnitude. That larger absolute depletion could greatly alter the relative depletions of phase A and phase B, if they enable phase A to primarily escape sputtering. This was an initial hope of Clayton's (1982) core-mantle construction. We also have ignored accretionary processes in the diffuse phase in our numerical results; but the observed depletions in diffuse clouds of poorly known ages may reflect also a history of depletion in those diffuse clouds themselves, and there may exist differential chemical sputtering and sticking of different elements. For these reasons we need not be dismayed that our study, primarily constructed to model the dust component during Galactic secular chemical evolution, does not—without further construction—explain the chemistry of the gas phase.

From solar system abundances (Anders and Ebihara 1982), we have

$$\frac{N_{\mathrm{Mg}}}{N_{\mathrm{Al}}} \approx 12.4\,,$$

whereas for ζ Ophiuchi (Spitzer 1978) $N_{\mathrm{Mg}}/N_{\mathrm{Al}} \approx 60$, where N_{X} is the abundance of element X relative to some standard, e.g., 10^6 Si atoms. Apparently Mg is fivefold less depleted compared with Al in that cloud, which is not atypical. We had hoped that our phase A/phase B core-mantle structure would accommodate those observations by the extra shielding of Al in the phase A cores.

TABLE 4

GRAIN POPULATION CHARACTERISTICS FOR CASE 3

Quantity	Value: SUNOCONs	Value: STARDUST	Value: Both
1. Number of particles injected $\{N_i\}$	1,534,029	628,383	2,162,412
2. Maximum size increment due to accretion $\{\Delta r\}$ (Å)	151	151	151
3. Number destroyed in the diffuse cloud $\{N_{d\,\mathrm{DC}}\}$	1,278,853	494,395	1,773,248
4. Number destroyed in the molecular cloud $\{N_{d\,\mathrm{MC}}\}$	182,762	71,112	253,874
5. Number surviving in the diffuse cloud $\{N_{s\,\mathrm{DC}}\}$	36,461	32,512	68,973
6. Number surviving in the molecular cloud $\{N_{s\,\mathrm{MC}}\}$	35,953	30,356	66,309
7. Total number surviving $\{N_f\}$	72,414	62,868	135,282
8. N_f/N_i (%)	4.72%	10.0%	6.26%
9. $N_{s\,\mathrm{DC}}/N_{s\,\mathrm{MC}}$	1.014	1.071	1.040
10. Total grain mass injected $\{M_{\mathrm{grain\ injected}}\}$ (kg)	1.17×10^{-13}	4.80×10^{-14}	1.65×10^{-13}
11. Total grain mass sputtered $\{M_{\mathrm{sputter}}\}$ (kg)	6.01×10^{-13}	2.43×10^{-13}	8.44×10^{-13}
12. Total grain mass astrated $\{M_{\mathrm{astrated}}\}$ (kg)	6.85×10^{-14}	2.74×10^{-14}	9.59×10^{-14}
13. Total mass accreted $\{M_{\mathrm{accreted}}\}$ (kg)	5.81×10^{-13}	2.44×10^{-13}	8.25×10^{-13}
14. Total surviving grain mass $\{M_{\mathrm{grain\ final}}\}$ (kg)	2.86×10^{-14}	2.16×10^{-14}	5.02×10^{-14}
15. Total final gas mass $\{M_{\mathrm{gas}}\}$ (kg)	...	...	1.91×10^{-14}
16. Total mass $\{M_{\mathrm{final}}\}$ (kg)	...	...	6.93×10^{-14}
17. $M_{\mathrm{final}}/M_{\mathrm{injected}}$	...	...	0.42
18. Grain mass in the diffuse cloud $\{M_{\mathrm{grain\ DC}}\}$ (kg)	9.44×10^{-15}	7.25×10^{-15}	1.67×10^{-14}
19. Grain mass in the MC $\{M_{\mathrm{grain\ MC}}\}$ (kg)	1.92×10^{-14}	1.44×10^{-14}	3.35×10^{-14}
20. $M_{\mathrm{gas}}/(M_{\mathrm{grain\ DC}} + M_{\mathrm{gas}})$	...	...	0.53
21. M_{final}/N_f (kg)	...	...	5.12×10^{-19}
22. $M_{\mathrm{injected}}/N_i$ (kg)	...	...	7.64×10^{-20}
23. $M_{\mathrm{sputter}}/M_{\mathrm{accreted}}$	1.03	1.00	1.02
24. $M_{\mathrm{sputter}}/M_{\mathrm{final}}$	8.67	3.51	12.18
25. $M_{\mathrm{astrated}}/M_{\mathrm{final}}$	0.99	0.90	1.39
26. $M_{\mathrm{accreted}}/M_{\mathrm{final}}$	8.38	3.52	11.90
27. Total mass of core injected $\{M_{\mathrm{A.injected}}\}$ (kg)	1.47×10^{-14}	5.99×10^{-15}	2.07×10^{-14}
28. Total mass of core sputtered $\{M_{\mathrm{A.sputter}}\}$ (kg)	1.03×10^{-14}	3.81×10^{-15}	1.41×10^{-14}
29. Total mass of core astrated $\{M_{\mathrm{A.astrated}}\}$ (kg)	3.08×10^{-15}	1.14×10^{-15}	4.22×10^{-15}
30. Total mass of core surviving $\{M_{\mathrm{A.final}}\}$ (kg)	1.25×10^{-15}	1.05×10^{-15}	2.30×10^{-15}
31. $M_{\mathrm{A.final}}/M_{\mathrm{A.injected}}$ (%)	8.5%	17.4%	11.1%
32. $M_{\mathrm{A.sputter}}/M_{\mathrm{A.injected}}$ (%)	70.5%	63.5%	68.1%
33. $M_{\mathrm{A.astrated}}/M_{\mathrm{A.injected}}$ (%)	21.0%	19.0%	20.4%
34. $M_{\mathrm{A.final}}/M_{\mathrm{final}}$ (%)	1.8%	1.5%	3.3%
35. $M_{\mathrm{A.injected}}/M_{\mathrm{injected}}$ (%)	12.5%	12.5%	12.5%
36. Mass of core-mantle injected $\{M_{\mathrm{B.injected}}\}$ (kg)	1.03×10^{-13}	4.20×10^{-14}	1.45×10^{-13}
37. Mass of core-mantle sputtered $\{M_{\mathrm{B.sputter}}\}$ (kg)	9.16×10^{-14}	3.62×10^{-14}	1.28×10^{-13}
38. Mass of core-mantle astrated $\{M_{\mathrm{B.astrated}}\}$ (kg)	8.04×10^{-15}	3.04×10^{-15}	1.11×10^{-14}
39. Mass of core-mantle surviving $\{M_{\mathrm{B.final}}\}$ (kg)	2.97×10^{-15}	2.76×10^{-15}	5.73×10^{-15}
40. $M_{\mathrm{B.final}}/M_{\mathrm{B.injected}}$ (%)	2.9%	6.6%	9.0%
41. $M_{\mathrm{B.sputter}}/M_{\mathrm{B.injected}}$ (%)	89.3%	86.2%	88.3%
42. $M_{\mathrm{B.astrated}}/M_{\mathrm{B.injected}}$ (%)	7.8%	7.3%	7.7%
43. $M_{\mathrm{B.final}}/M_{\mathrm{final}}$ (%)	4.3%	4.0%	8.3%
44. $M_{\mathrm{B.injected}}/M_{\mathrm{injected}}$ (%)	87.5%	87.5%	87.5%
45. $M_{\mathrm{B.injected}}/M_{\mathrm{A.injected}}$	7.00	7.00	7.00
46. $M_{\mathrm{B.final}}/M_{\mathrm{A.final}}$	2.39	2.64	2.49

Our program injects grains having the initial mass ratio $M_B/M_A = 7$. At a time 6 Gyr, we can determine the mass ratio of B to A for material in the mantle and gas by mass balance using the mass of A and B material that still remains. For example, in Table 2 (line 34) 9.83% of all A material still resides untouched in the A core, while (from line 43) 3.45% of all B material is present in the B mantle. The remainder must be in the accreted C mantles and in the gas. Whether the C mantles and the gas differ in composition or not will depend upon whether the specific elements involved (in this case Al in A and Mg in B, initially) are sputtered with equal efficiency from grain surfaces and whether they have equal sticking probabilities in collisions with grains. In the interest of presenting this more complete approach to chemical evolution, we find it reasonable to, at first, assume equal sputtering and sticking efficiencies, so that C mantles and gas have almost the same composition, which in that case is

$$\left(\frac{M_B}{M_A}\right)_{\mathrm{ISM}} = \frac{7(1 - 0.0345)}{1 - 0.0983} = 7.5 , \tag{26}$$

which is not significantly greater than the bulk initial abundance ratio of 7. Since almost all of both phases A and B have been sputtered at some time, the abundances in the reaccreted mantles and in the gas must be in this simple model approximately normal. As it stands, the model does not account for the observed greater Al depletion factors. To achieve agreement in this way requires greater shielding of phase A cores.

c) *Lifetimes and Anomalies*

Given the nature of our computer codes, where we can follow the development of each dust particle, it is possible to

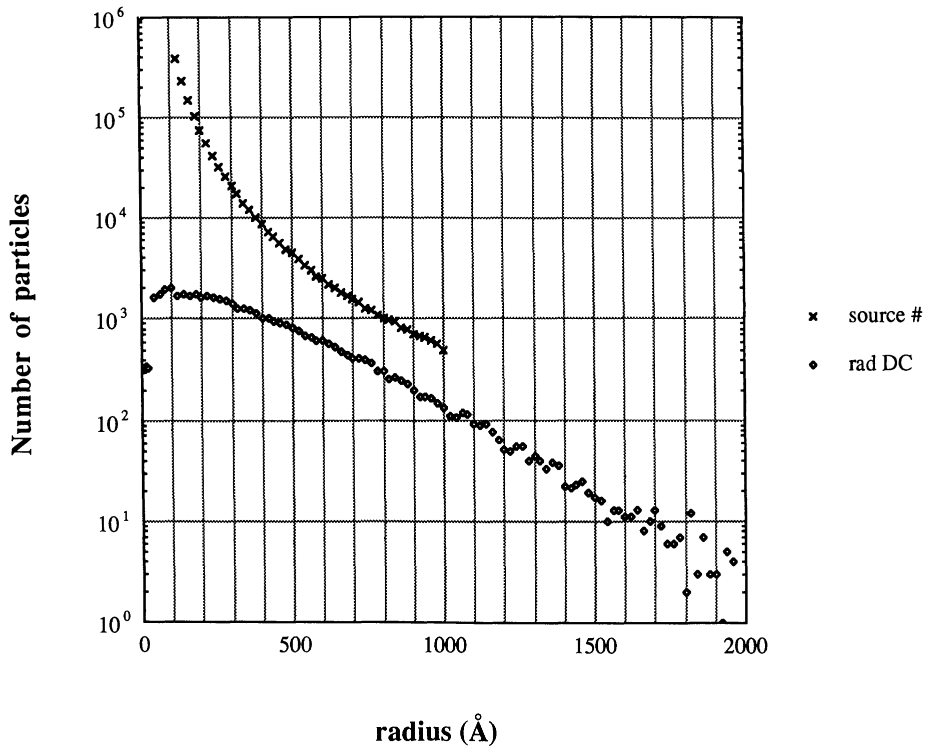

FIG. 7.—Number of particles versus the radius of the particles for the total number of injected dust grains over 6 Gyr (*crosses*) and the evolved dust spectrum in the diffuse clouds (*open squares*) at $t = 6$ Gyr for case 2. The largest dust grains reach a radius of over 2000 Å, and, since the maximum thickness of the accreted mantle is 178 Å (see Fig. 5*b* and Table 3), we can see that the dust grains have cycled through the different phases of the ISM at least 5 times. In this example 1,260,321 grains were injected into the ISM over 6 Gyr, and 46,518 were found to have survived in the diffuse medium when the program finished. The evolved grain-size distribution may be described approximately by the equation $4000 \exp(-r/280)$.

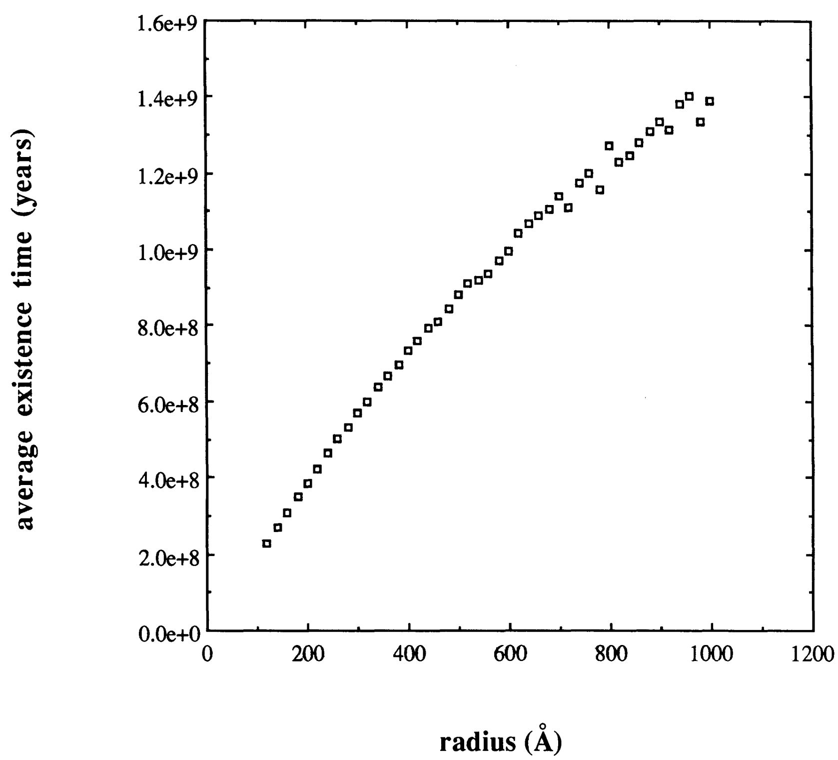

FIG. 8.—Average existence time for case 1 of the dust grains as a function of their initial sizes, which were arbitrarily restricted to the injection range 100 Å $< a <$ 1000 Å.

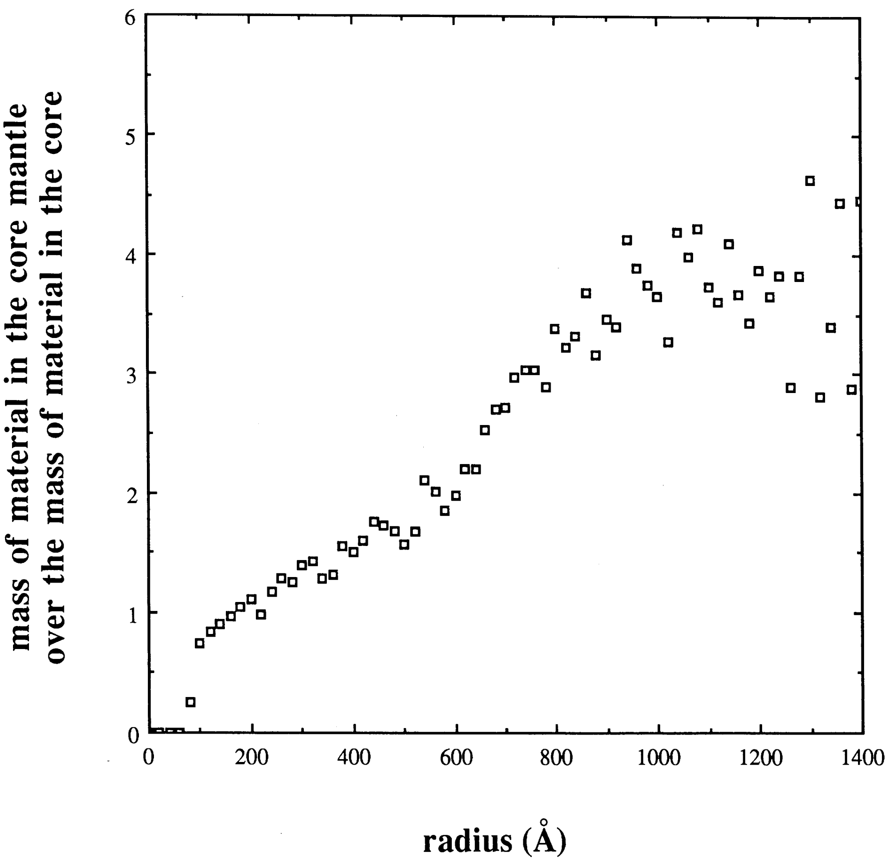

FIG. 9.—Mass ratio of the B shell to the A core as a function of the total radius of the dust grain for case 2. The initial value of this ratio for all injected particles is constructed to be equal to 7. Note that the statistical scatter in the data points increases as the radii of the particles increase, this being due to the small number of particles that reach sizes greater than 1000 Å.

obtain the average lifetime of a particle as a function of its initial radius. A graphical depiction of these results is shown in Figure 8. The lifetimes shown here are the actual times that the particles existed before being destroyed (averaged over all particles having the same initial size). The distinction between the existence lifetime and the mass lifetime [$=m/(dm/dt)$, where m is the mass of dust in the ISM and dm/dt is the rate of sputtering] is an important one in discussions of isotopic anomalies. Expanded discussion of this distinction may be found in Liffman and Clayton (1988). The particles live much longer than the mass turnover time, because the history of evolved dust in our calculations is overwhelmingly that of successive sputtering and reaccretion of phase C mantles overlying the remnants of the initial refractory core-mantle particles.

One sees from Figure 8 that the average existence time of the dust grains in a constant sputtering rate environment is a function of the initial size of the dust grains, where the smallest initial particles of 100 Å radius are destroyed in approximately 2×10^8 yr, while the large 1000 Å particles last for around 1.4×10^9 yr—even though the mass-sputtering lifetime of a 1000 Å dust grain in the diffuse media is only 5×10^8 yr. The lifetime distribution obtained in Figure 8 is by no means unique. It is a heavily dependent function of the physical environment in the interstellar medium. For example, Liffman and Clayton (1988) used in some of their trials an inertial sputtering mechanism and found that the lifetimes of the dust grains were not then dependent on the initial size of the dust grains. The average sputtering in the real ISM is probably a complicated mixture of thermal and inertial sputtering, to which must be added fragmentation and vaporization in grain-grain collisions.

The results from Tables 2–4 tell us that approximately 10% by mass of the initial core material survives the interstellar processes—much more than the 1% expected from a simple mean rate calculation (Liffman and Clayton 1988). It is clear that the mantle, which is accreted onto the dust grain as it goes from the diffuse medium to the molecular cloud, acts as a protector of the inner core of the dust grain and may thus protect any isotopically anomalous material that is present. Indeed it is even possible to fractionate the isotopes that are present in the dust grain, via the processes of sputtering and accretion. This is shown in Figure 9. Here we see that M_B/M_A is an increasing function of the grain size. This means that large and small particles can differ in isotopic composition if the phases A and B have different isotopic composition, as they can in SUNOCONs. It is very interesting that the injected particles have, by construction, identical isotopic compositions with $M_B/M_A = 7$ for all particles and that Galactic evolution has produced isotopic fractionation according to grain size, an effect pointed out by Clayton (1980). It is equally interesting that if the Al in phase A SUNOCON cores is injected as ^{16}O-pure oxides, that correlation remains at about the 10% level even after 6 Gyr, suggesting that it is indeed a viable cause of the observed correlation in meteorites of ^{16}O excess with aluminum (in the sense that the ^{16}O-rich samples are Al-rich inclusions). Liffman and Clayton (1988) have discussed these and other applications to the isotopic anomaly problem, and we will not elaborate here.

If it were possible to place the smaller dust grains (e.g., grains with sizes less than 500 Å) in a different section of the presolar nebula from the larger dust grains—as has been proposed by Elmegreen (1979)—then M_B/M_A would become a function of position within the presolar nebula. When one considers that the A core and B shell of our dust grains contain different elements, e.g., aluminum in the A core and magnesium in the B shell, then it is clear that the elemental ratios of these elements would vary throughout the presolar nebula.

d) Criticisms and Conclusions

The simulation that has been outlined in the preceding pages should be regarded as only a first, halting step in the simulation of the interstellar dust system (IDS). Our purpose has been to illuminate the basic features of that system and also to cast it into the chemical evolution framework. Clearly there are many criticisms that can be made of our approach, only a few of which we will outline here:

1. We have neglected the role of shock-produced grain-grain fragmentation, which may have a major influence on the IDS evolution.

2. In only considering the very refractory elements such as aluminum and magnesium, we have neglected the refractory carbonaceous component of interstellar dust. This component may provide a shielding mantle for the other refractory elements (Si, Ca, Fe, etc.), which have properties similar to the phase A and phase B condensates.

3. If the dust grains survive long enough, they will repeatedly traverse the molecular clouds, thereby obtaining several layers of accretionary mantle. The isotopic composition of these different mantles will be a function of time owing to nucleosynthetic processes and to the evolution of the IDS (Clayton and Pentalaki 1986; Clayton 1988). Thus any accurate simulation of the IDS must allow the dust grain to accrete various layers of mantle and keep track of the elemental and isotopic composition of each layer. Such a simulation will allow for the accurate determination of the elemental abundances in each of the separate phases of the ISM.

Noting all these caveats, we can conclude that roughly 10% of the superrefractory material survives the rigors of our interstellar medium intact (thus providing a transport mechanism for any isotopically anomalous material that may have been present when the dust first formed). We also find that the calculated average sputtering rates that we have adopted maintain far more refractory gas in the diffuse phase than is observed. The remedies for this are one or all of the following: sputtering rates are smaller; substantial accretion occurs also in the diffuse medium, especially in the clouds observed; and/or refractory atoms are sputtered less rapidly owing to greater shielding by carbonaceous mantles. Our hope is to investigate these possibilities in future studies addressing the gas composition.

This research was supported in part by the Robert A. Welch Foundation and in part by NASA grant NAG-9-100 BASIC.

APPENDIX

THE ACCRETION EQUATION

The accretion equation is obtained by considering a transit cloud of gas and dust that is in the process of being transferred from the diffuse media to a molecular cloud. After this transferring material has been incorporated into the molecular cloud, a mass M of gas that was contained in the transit cloud will have condensed onto k dust grains that were also in the transit cloud, and, as discussed in § III of this paper, all of the dust grains will obtain the same thickness of accreted material (Δr) irrespective of the initial size of the individual dust grain as it entered the molecular cloud.

We thus have, for spherical dust grains,

$$M = \sum_{i=1}^{k} \left[\frac{4\pi}{3}(r_i + \Delta r)^3 - \frac{4\pi}{3} r_i^3\right]\rho_g = \frac{4\pi}{3} k\rho_g\left[3\Delta r\langle r_i^2\rangle + 3(\Delta r)^2\langle r_i\rangle + (\Delta r)^3\right]. \tag{A1}$$

If we now assume that the transit cloud was a sample from a uniform, well-mixed diffuse medium, then the mean radius of the dust grains in the transit cloud ($\langle r_i\rangle$) will be equal to the mean radius of dust grains in the diffuse cloud ($\langle r\rangle_{DC}$). Similarly $\langle r_i^2\rangle = \langle r^2\rangle_{DC}$ and M/k in the diffuse medium equals M/k in the transit cloud. Thus we can write

$$(\Delta r)^3 + 3(\Delta r)^2\langle r\rangle_{DC} + 3\Delta r\langle r^2\rangle_{DC} - \frac{3M}{4\pi k\rho_g} = 0\,, \tag{A2}$$

where the quantities are now defined as in § III. It turns out that the inequality $\langle r^2\rangle \geq \langle r\rangle^2$ (which is always true) implies that equation (A2) has only one real solution.

REFERENCES

Anders, E., and Ebihara, M. 1982, *Geochim. Cosmochim. Acta*, **46**, 2362.
Chandrasekhar, S. 1943, *Rev. Mod. Phys.*, **51**, 1.
Clayton, D. D. 1978, *Moon and Planets*, **19**, 109.
———. 1980, *Earth Planet. Sci. Letters*, **47**, 199.
———. 1982, *Quart. J.R.A.S.*, **23**, 174.
———. 1984, *Ap. J.*, **285**, 411.
———. 1988, *Ap. J.*, **334**, 191.
Clayton, D. D., and Pentalaki, I. 1986, *Ap. J.*, **307**, 441.
Cowie, L. L., and Songaila, A. 1986, *Ann. Rev. Astr. Ap.*, **24**, 499.
Draine, B. T., and Salpeter, E. E. 1979*a*, *Ap. J.*, **231**, 77.
———. 1979*b*, *Ap. J.*, **231**, 438.
Elmegreen, B. G. 1979, *Ap. J.*, **232**, 729.
Field, G. B. 1974, *Ap. J.*, **187**, 453.
Greenberg, J. M. 1978, in *Cosmic Dust*, ed. J. A. M. McDonnell (New York: Wiley), p. 187.
Grossman, L., and Larimer, J. 1974, *Rev. Geophys. Space Phys.*, **12**, 71.
Liffman, K. 1988, Ph.D. thesis, Rice University.
Liffman, K., and Clayton, D. D. 1988, *Proc. Lunar Planet. Sci. Conf.*, **18**, 637.
Mathis, J. S. 1985, NASA CP-2403, p. 29.
Mathis, J. S., Rumpl, W., and Nordsieck, K. H. 1977, *Ap. J.*, **279**, 425.
Rowan-Robinson, M. 1986, *M.N.R.A.S.*, **219**, 737.
Salpeter, E. E. 1977, *Ann. Rev. Astr. Ap.*, **15**, 267.

Seab, C. G., and Shull, J. M. 1983, *Ap. J.*, **275**, 652.
Shull, J. M. 1978, *Ap. J.*, **226**, 858.
Spitzer, L., Jr. 1978, *Physical Processes in the Interstellar Medium* (2d ed.; New York: Wiley).
Tielens, A. G. G. M., Seab, C. G., Hollenbach, D. J., and McKee, C. F. 1987, *Ap. J.* (*Letters*), **319**, L109.
Tinsley, B. M. 1980, *Fund. Cosmic Phys.*, **5**, 287.

DONALD D. CLAYTON: Department of Space Physics and Astronomy, Rice University, Houston, TX 77251

KURT LIFFMAN: MS 245-3, NASA Ames Research Center, Moffett Field, CA 94035